Thermal Reactions of Isodihydrobenzofuran: Experimental Results and Computer Modeling

Assa Lifshitz,* Aya Suslensky, and Carmen Tamburu

Department of Physical Chemistry, The Hebrew University of Jerusalem, Jerusalem 91904, Israel

Received: August 29, 2000; In Final Form: November 15, 2000

The thermal reactions of isodihydrobenzofuran (phthalan) were studied behind reflected shock waves in a single pulse shock tube over the temperature range 1050−1300 K and overall densities of $\sim 3 \times 10^{-5}$ mol/cm^3. The total decomposition rate, expressed as a first-order rate constant, is $10^{12.10}$ exp($-53.7 \times 10^3/RT$) s^{-1}, where R is in given units of cal/(K mol). One isomerization product, *o*-tolualdehyde [$k_{\text{isomerization}} = 10^{16.50}$ exp ($-80.5 \times 10^3/RT$) s^{-1}], and products resulting from unimolecular cleavage of the furan ring were obtained under shock heating. Carbon monoxide and toluene are the products of the highest concentration. Isobenzofuran is obtained by a 1,6-H_2 elimination from the furan ring with a rate constant $k = 10^{13.78}$ exp($-70.0 \times 10^3/RT$) s^{-1}. In addition, benzene, ethylbenzene, styrene, ethylene, methane, and acetylene were found in the postshock mixtures. Trace quantities of allene and propyne were also found. In addition to H-atom ejection from the furan ring, it is believed that phthalan decomposes via two unimolecular reactions that involve cleavage of the furan ring. One reaction yields stable products, phthalan → C_6H_5-CH_3 + CO [$k = 10^{14.11}$ exp($-67.0 \times 10^3/RT$) s^{-1}], and one decomposition yields unstable intermediates which are responsible for the propagation of free radical reactions in the system, phthalan → HCO$^\bullet$ + C_6H_5-$CH_2^\bullet$ ($k = 10^{16.6}$ exp($-78.0 \times 10^3/RT$) s^{-1}). A reaction scheme containing 26 species and 49 elementary reactions was constructed, and computer modeling was performed in 25 K intervals over the range 1050−1300 K. The agreement between the experimental and the calculated yields is reasonable. Differences and similarities in the thermal behavior of isodihydrobenzofuran, dihydrobenzofuran, 2,3-dihydrofuran, and 2,5-dihydrofuran and the effect of fused benzene ring are discussed.

Introduction

The thermal reactions of the furan ring, with and without substituents, have been the subject of extensive experimental and theoretical (quantum mechanical) investigations. Tetrahydrofuran is a kinetically stable 5-membered ring compound that undergoes ring cleavage with a high activation energy (~83 kcal/mol) to yield mainly ethylene and ketene and formaldehyde and propylene.[1] With the introduction of partial unsaturation to the ring the two isomers 2,5-dihydrofuran and 2,3-dihydrofuran are obtained. These molecules are considerably less stable than tetrahydrofuran and decompose at much lower temperatures. 2,3-Dihydrofuran isomerizes and decomposes simultaneously[2,3] whereas the main reaction in 2,5-dihydrofuran is a H_2 elimination to form furan[4,5] and no isomerization is observed. With an additional double bond the furan molecule is formed. This is again a very stable molecule that decomposes at higher temperatures to yield mainly methylacetylene and carbon monoxide.[6−9] The thermal reactions of furonitrile,[10] 2-methylfuran,[9,11] and 2,5-dimethylfuran[12] have also been investigated, and the effects of the substituents on the reactions of the ring were examined. Ruifeng Liu et al.[13] and Bouchoux et al.[14] performed detailed ab initio quantum mechanical calculations on the various decomposition channels of furan.

Recently, the decompositions of indene[15] and indole[16] were investigated using the single pulse shock tube technique, to examine the effect of fused benzene ring on the thermal reactions of the 5-membered ring. In these two compounds benzene replaces a double bond in cyclopentadiene and pyrrole. A considerable stabilization of the 5-membered ring was evident. We have recently published a detailed investigation on the thermal reactions of 2,3-dihydrobenzofuran.[17]

We present here a detailed investigation on the thermal reactions of isodihydrobenzofuran (phthalan) and compare the isomerization reactions and the decomposition channels of the dihydrofurans to the dihydrobenzofurans.

Experimental Section

Apparatus. The thermal reactions of isodihydrobenzofuran were studied behind reflected shock waves in a pressurized driver 2 in. i.d single pulse shock tube. The tube, made of electropolished stainless steel tubing, was heated and maintained at 170 °C with an accuracy of ±1 °C. The driven section was 4 m long and was divided in the middle by a 2 in. i.d. ball valve. The driver had a variable length up to a maximum of 2.7 m and could be varied in small steps in order to tune for the best cooling conditions. A 36-L dump tank was connected to the driven section near the diaphragm holder in order to prevent reflection of transmitted shocks and in order to reduce the final pressure in the tube before collecting a sample for analysis. The driven section was separated from the driver by Mylar polyester film of various thickness depending upon the desired shock strength.

After the tube was pumped down to approximately 10^{-5} Torr, the reaction mixture was introduced into the section between the ball valve and the end plate of the driven section, and pure argon into the section between the diaphragm and the valve, including the dump tank. After a shock was fired, gas samples were transferred directly from the tube through an outlet in the

10.1021/jp003093f CCC: $20.00
Published on Web 02/22/2001

driven section (near the end plate) into Hewlett-Packard model 5890A gas chromatographs using flame ionization (FID) detectors. All the connecting tubes were heated to 170 °C.

Reflected shock temperatures were determined from the extent of decomposition of 1,1,1-trifluoroethane, which was added in small quantities to the reaction mixtures to serve as an internal standard. Its decomposition to $CH_2{=}CF_2 + HF$ is a first-order unimolecular reaction that under the temperature and pressure conditions of this investigation has a rate constant of[18] $k_{first} = 10^{14.85} \exp(-74.05 \times 10^3/RT)\ s^{-1}$. Reflected shock temperatures were calculated from the relation

$$T = -(E/R)\Big/\left[\ln\left\{-\frac{1}{At}\ln(1-\chi)\right\}\right]$$

where t is the reaction dwell time, A and E are the preexponential factor and the activation energy of the standard reaction, and χ is the extent of decomposition defined as

$$\chi = [CH_2{=}CF_2]_t/([CH_2{=}CF_2]_t + [CH_3CF_3]_t)$$

Density ratios behind the reflected shock waves were calculated from the measured incident shock velocities using the three conservation equations and the ideal gas equation of state. The incident shock velocities were measured with two, miniature, high-frequency−high-temperature pressure transducers (PCB model M113M199) placed 300 mm apart, near the end plate of the driven section. The signals generated by the shock waves passing over the transducers were fed through a piezo amplifier to a Nicolet model 3091 digital oscilloscope. Time intervals between the two signals shown on the oscilloscope were obtained digitally with an accuracy of ±2 μs, corresponding to approximately ±15 K. A third transducer placed in the center of the end plate of the driven section provided measurements of the reaction dwell times (approximately 2 ms) with an accuracy of ±5%. Cooling rates were approximately 5×10^5 K/s.

Materials and Analysis. Reaction mixtures containing 0.3% phthalan and 0.08% 1,1,1-trifluoroethane diluted in argon were prepared and stored at 1 atm in 12-L glass bulbs. The bulbs and the gas handling manifold were maintained at 170 °C and were pumped down to ~10^{-5} Torr. The reactants were obtained from Aldrich Chemical Co., Inc., and were of high purity. The argon used was Matheson ultrahigh purity grade, listed as 99.9995%, and the helium was Matheson pure grade, listed as 99.999%. All the materials were used without further purification.

The gas chromatographic analyses of the products in the postshock mixtures (except for CO) were performed on a Porapak N column using a flame ionization detector. The column's initial temperature of 35 °C was gradually elevated to 190 °C in analyses which lasted over 2 h. A typical chromatogram of 0.3% phthalan in argon shock heated to 1215 K (not including CO) is shown in Figure 1. The Porapak N column could not separate benzaldehyde from isobenzofuran. They were determined quantitatively with the aid of a GC/MS using different m/z peaks of their spectrum.

Carbon monoxide was analyzed on a 2 m molecular sieve 5A column at 35 °C. It was reduced at 400 °C to methane prior to its detection using a Chrompak methanyzer with a carrier gas composed of 50% hydrogen and 50% argon. These analyses gave the ratio $[CO]/[CH_3CF_3]$. From these ratios and the known concentration of 1,1,1-trifluoroethane obtained in the Porapak N analyses, the concentration of CO could be determined for each run. The ratio $[CO]/[CH_3CF_3]$ in a standard mixture of

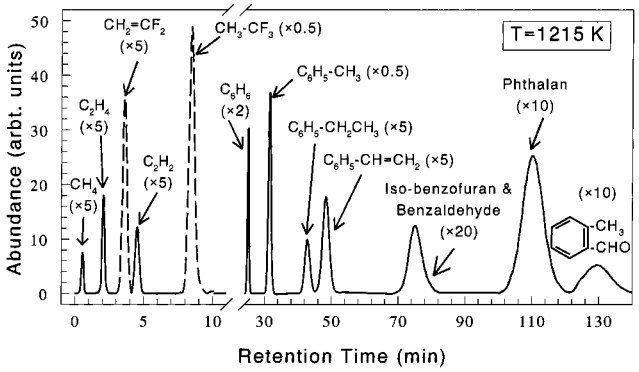

Figure 1. Gas chromatogram of a shock-heated sample of 0.3% phthalan and 0.08% 1,1,1-trifluoroethane in argon, to 1215 K. The numbers on the chromatogram are multiplication factors.

1,1,1-trifluoroethane and carbon monoxide was determined periodically in order to verify a complete conversion of these two compounds to methane in the methanyzer.

Identification of the reaction products was based on their retention times in the gas chromatograph. It was also assisted by GC/MS measurements carried out on a Hewlett-Packard model 5970 Mass Selective Detector. The sensitivities of the reaction products were determined from standard mixtures. The areas under the GC peaks were integrated with Spectra Physics model SP4200 computing integrators and were transferred to a PC for data reduction and graphical presentation.

Evaluation of the Product Concentrations. When a large number of products are formed as a result of shock heating, the evaluation of the absolute concentrations of the reaction products from the area under their GC peaks is more complicated. To avoid errors resulting from irreproducibility of the detectors, concentrations of reaction products $C_5(pr)_i$ were calculated relative to the concentration of the reactant. Evaluation of the concentrations of the individual products from their GC peak areas were done using the following relations:

$$C_5(pr)_i = A(pr_i)_t/S(pr_i)\{C_5(\text{reactant})_0/A(\text{reactant})_0\}$$

$$C_5(\text{reactant})_0 = \{p_1(\%\ \text{reactant})(p_5/p_1)/100RT_1\}$$

$$A(\text{reactant})_0 = A(\text{reactant})_t + (1/N)\Sigma[n(pr_i)A(pr_i)/S(pr_i)]$$

$C_5(\text{reactant})_0$ is the concentration of a reactant behind the reflected shock prior to decomposition, $A(\text{reactant})_0$ is its calculated GC peak area prior to decomposition, and N is the number of its carbon atoms, 8 in isodihydrobenzofuran. $A(pr_i)_t$ is the peak area of a product i in the shocked sample, $S(pr_i)$ is its sensitivity relative to reactant, and $n(pr_i)$ is the number of its carbon atoms. p_5/p_1 is the compression behind the reflected shock wave, and T_1 is the temperature of the reaction mixture prior to shock heating, i.e. the temperature of the shock tube, 170 °C in the present study.

Results

To determine the distribution of reaction products, some 35 tests were run with mixtures containing 0.3% isodihydrobenzofuran and 0.08% 1,1,1-trifluoroethane in argon. The temperature range covered was ~1070−1300 K at overall densities of $(2.5-3) \times 10^{-5}$ mol/cm^3. Details of the experimental conditions and the distribution of reaction products are given in Table 1 and are shown as an overview in Figure 2. Figure 2a

TABLE 1: Experimental Conditions and Product Distribution (in mol %) in the Decomposition of Isodihydrobenzofuran

no.	T_5	10^5C_5	phthalan	CO	$C_6H_5CH_3$	*o*-tolualdehyde	styrene	C_6H_6	$C_6H_5C_2H_5$	benzaldehyde	isobenzofuran	C_2H_4	C_2H_2	CH_4
1	1066	2.89	95.33	2.61	1.59	0.126	0.149	0.098	0.028	0.025	0.026			0.014
2	1087	2.38	92.45	3.14	3.58	0.146	0.221	0.119	0.031	0.141	0.104	0.024		0.046
3	1098	2.86	93.93	2.77	2.51	0.220	0.224	0.143	0.047	0.083	0.054	0.00065		0.014
4	1104	2.04	88.73	5.30	3.57	0.443	0.241	0.651	0.144	0.527	0.323	0.070		
5	1104	2.66	86.06	7.83	3.84	0.795	0.316	0.455	0.121	0.302	0.184	0.038		0.060
6	1118	2.72	85.43	5.93	6.43	1.12	0.483	0.200	0.060	0.182	0.097	0.031	0.035	
7	1122	2.70	82.91	8.44	5.12	1.34	0.410	0.592	0.179	0.574	0.298	0.060		0.078
8	1141	2.23	76.2	11.96	7.45	1.33	0.623	1.16	0.313		0.652	0.159		0.155
9	1141	2.63	80.20	9.77	7.43	1.19	0.527	0.307	0.164	0.255	0.126	0.035		
10	1143	2.69	74.85	10.62	9.49	1.42	0.718	1.01	0.350	0.783	0.388	0.106	0.190	0.081
11	1143	2.63	81.72	9.19	5.88	0.954	0.457	0.581	0.192	0.563	0.279	0.050	0.091	0.041
12	1146	2.52	74.63	12.09	8.31	1.31	0.720	0.944	0.322	0.909	0.450	0.085	0.157	0.079
13	1153	2.30	72.89	13.52	8.37	2.17	0.657	0.765	0.267	0.716	0.360	0.081	0.136	0.065
14	1155	2.49	76.55	10.82	8.21	2.25	0.625	0.427	0.238	0.482	0.243	0.053	0.059	0.041
15	1159	2.55	73.34	11.69	10.33	2.88	0.80	0.490	0.290			0.061	0.065	0.046
16	1168	2.30	58.39	17.57	15.23	3.60	1.14	1.17	0.516	1.30	0.718	0.134	0.153	0.093
17	1171	2.15	61.05	19.62	11.49	2.81	0.995	1.29	0.483	1.14	0.638	0.152	0.241	0.104
18	1179	2.47	55.30	20.53	14.90	3.02	1.33	1.58	0.696	1.40	0.844		0.276	0.126
19	1181	2.12	73.55	12.01	5.88	4.67	0.687	0.684	0.330	1.18	0.724	0.095	0.142	0.051
20	1183	2.38	68.89	12.69	7.48	4.09	0.474	1.44	0.544	2.60	1.62		0.172	
21	1200	2.39	48.81	15.55	20.42	8.07	2.29	1.34	1.0	1.20	0.880	0.20	0.138	0.108
22	1202	2.75	53.55	17.69	15.29	8.70	1.57	0.886	0.723	0.902	0.674			
23	1211	2.43	45.23	19.02	19.09	8.47	2.20	1.72	0.974	1.50	1.22	0.241	0.178	0.161
24	1215	2.14	26.93	30.42	24.91	5.86	2.92	2.44	1.304	2.24	1.93	0.411	0.402	0.240
25	1226	2.48	49.09	17.30	15.89	9.34	2.29	1.19	0.868	2.08	1.98			
26	1246	2.34	27.67	27.69	23.12	10.37	3.26	2.24	1.19	1.76	1.96	0.416		0.301
27	1246	2.58	27.29	26.71	23.56	12.25	3.0	2.01	1.23	1.57	1.74	0.20	0.335	0.111
28	1249	2.19	30.15	32.0	20.36	8.37	2.27	1.81	1.04	1.49	1.69	0.218	0.474	0.138
29	1252	2.29	19.71	33.33	27.46	5.98	3.27	3.01	1.51	2.33	2.70		0.574	0.135
30	1253	2.17	10.56	39.31	28.13	5.03	3.71	4.19	1.45	2.73	3.21	0.273	0.974	0.423
31	1269	2.42	17.05	29.67	28.16	12.66	3.37	2.64	1.33	1.97	2.72		0.432	
32	1270	2.00	12.79	37.31	21.81	5.24	3.17	5.05	2.25	3.74	5.11	0.605	2.016	0.913
33	1293	2.03	6.89	37.66	30.01	5.14	4.37	4.85	1.11	2.59	4.12	0.349	2.187	0.728
34	1298	2.39	8.73	33.80	29.94	11.07	3.97	3.55	1.20	2.15	3.71		1.491	0.387

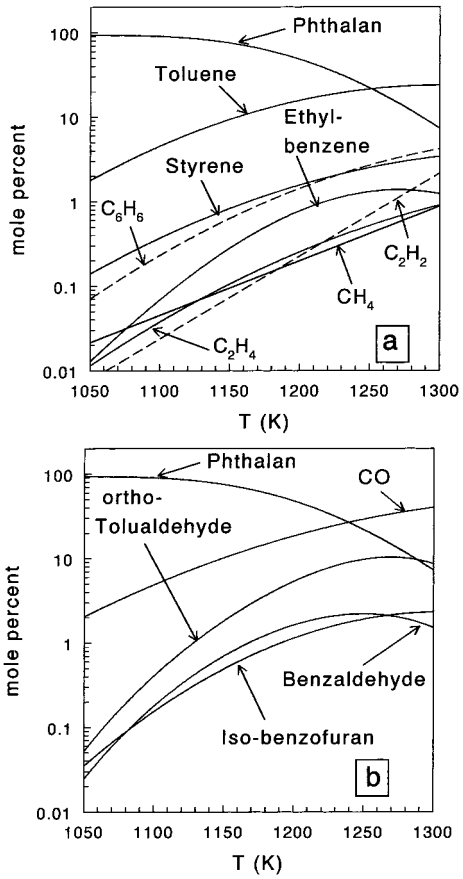

Figure 2. Product distribution: (a) without oxygen; (b) with oxygen.

shows all the reaction products that do not contain oxygen, and Figure 2b, those that do contain oxygen. As can be seen, carbon monoxide and toluene are the products of the highest concentration. Both are believed to be formed in the reaction

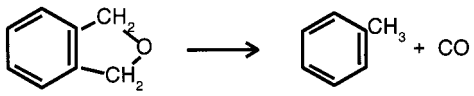

However, the concentrations of carbon monoxide are higher than those of toluene since there are other channels that produce CO, particularly $HCO^{\bullet} \rightarrow CO + H^{\bullet}$.

In addition to the products shown in Figure 2, trace quantities of allene, propyne, ethane, C_4H_4, C_4H_2, and others were found among the reaction products. Since their concentrations were very minute, they are not reported as part of the general product distribution.

Figure 3 shows an Arrhenius plot of the total decomposition of isodihydrobenzofuran. The rate constants on the graph are calculated as a first-order rate constants using the relation

$$k_{\text{total}} = -\ln\{[\text{isodihydrobenzofuran}]_t/[\text{isodihydrobenzofuran}]_0\}/t$$

The value obtained is $k_{\text{total}} = 10^{12.10} \exp(-53.7 \times 10^3/RT)\ \text{s}^{-1}$, where R is expressed in units of cal/(K mol). It should be mentioned that the total decomposition of isodihydrobenzofuran is not a first-order process. The first-order rate constant gives, however, a good estimate of the total decomposition rate over the temperature range covered in this investigation.

Figures 4 and 5 show Arrhenius plots for two unimolecular reactions that take place in the decomposition of isodihydrobenzofuran: the isomerization of isodihydrobenzofuran to *o*-tolualdehyde and the 1,6-H_2 elimination from isodihydroben-

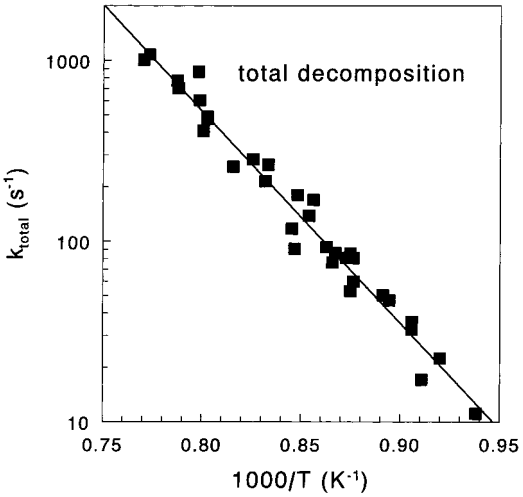

Figure 3. Arrhenius plot for the total decomposition of phthalan.

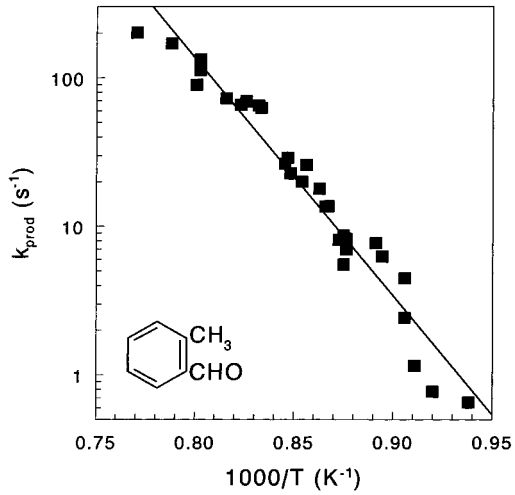

Figure 4. Arrhenius plot for production (formation minus decomposition) of the isomerization product *o*-tolualdehyde.

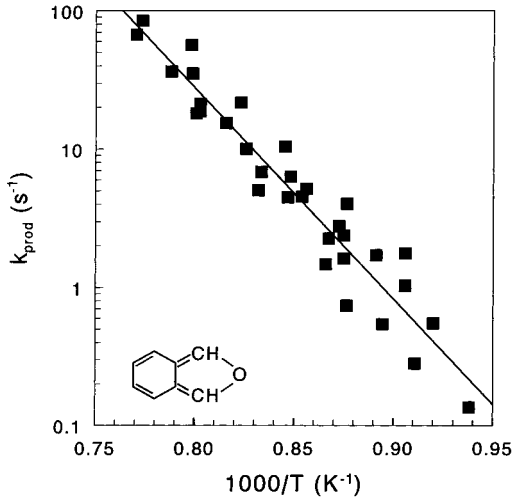

Figure 5. Arrhenius plot for production (formation minus decomposition) of isobenzofuran.

zofuran to form isobenzofuran. Their rate constants are calculated from the relation

$$k_{\text{product}} = \frac{[\text{product}]_t}{[\text{reactant}]_0 - [\text{reactant}]_t} k_{\text{total}}$$

TABLE 2: Arrhenius Parameters for the Decomposition of Isodihydrobenzofuran

compd	log (A, s^{-1})	E (kcal/mol)	compd	log (A, s^{-1})	E (kcal/mol)
tot. decomposn	12.10	53.7	benzaldehyde	12.03	60.2
CO	11.03	48.4	isobenzofuran	13.65	69.8
toluene	11.15	49.6	ethylbenzene	12.40	64.2
o-tolualdehyde	15.12	73.2	C_2H_2	13.79	73.7
styrene	11.90	59	CH_4		
benzene	12.30	61.8	C_2H_4	11.25	60.6

It should be stressed again that both the preexponential factors and the activation energies, which are obtained from the plots for these two reactions, are lower than the true values owing to further decomposition and the existence of parallel channels.

Values of E obtained from the slopes of the Arrhenius lines for product formation and their corresponding preexponential factors are summarized in Table 2 for all the products, including those whose production is associated with free radical reactions. For the latter, obviously, the Arrhenius parameters do not correspond to the parameters of true first-order rate constants. They do provide, however, a convenient way to summarize general rates. Even for the unimolecular reactions of the reactant, the parameters are not precisely those of the single reaction owing to further decomposition and parallel production channels.

Discussion

Unimolecular and Free Radical Reactions. Among the reactions that characterize the decomposition of isodihydrobenzofuran, there are four unimolecular reactions that isodihydrobenzofuran undergoes. In all the four reactions the benzene ring stays intact and changes occur only in the furan ring. Three reactions are associated with cleavage of the furan ring, and in one, molecular hydrogen is eliminated. There is one isomerization reaction in which hydrogen migrates from position 3 to position 1 in the ring and the C(1)−O(2) bond is broken to yield *o*-tolualdehyde.

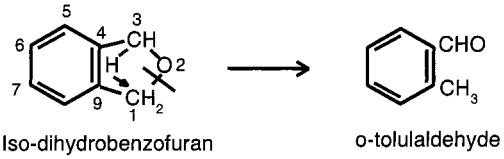

In another reaction, hydrogen molecule is eliminated from the 1,3 positions in the furan ring in a 1,6-elimination process to yield isobenzofuran.

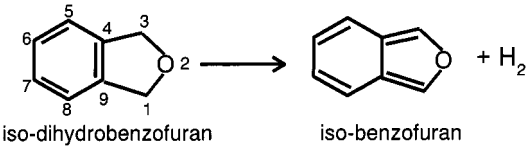

There are two additional reactions in which the furan ring is cleaved to yield two products: toluene + carbon monoxide and benzyl• + HCO•.

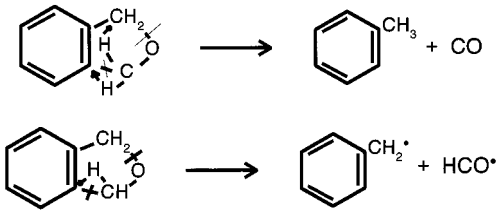

TABLE 3: Reaction Scheme for the Decomposition of Isodihydrobenzofuran

No	Reaction	A (s^{-1})	E (kcal)	k_f(1150 K)	k_r(1150 K)	ΔS_r(1150 K)	ΔH_r(1150 K)	Reference
1	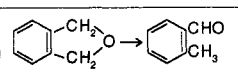	3.16×10^{16}	80.5	15.9	1.40×10^{-3}	14.2	0.194	This invest
2	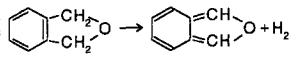	6.0×10^{13}	70	3	2.0×10^{4}	35.8	47.1	This invest
3	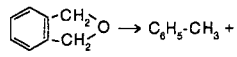	1.30×10^{14}	67	24.1	2.2×10^{-4}	44.3	−1.80	This invest
4	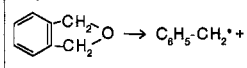	4.0×10^{16}	78	60.2	2.21×10^{9}	53	74.6	est
5	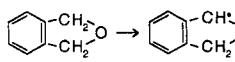	6.0×10^{15}	85	0.422	1.31×10^{14}	32.3	87.2	est
6	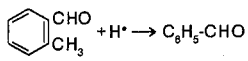	4.80×10^{13}	5.10	5.15×10^{12}	9.02×10^{8}	5.31	−13.7	est
7	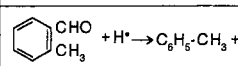	4.80×10^{13}	5.10	5.15×10^{12}	7.64×10^{7}	5.11	−19.5	est
8	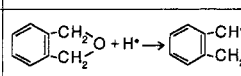	7.0×10^{13}	15	9.88×10^{10}	1.75×10^{6}	4.83	−19.4	est
9	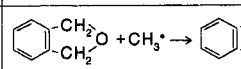	1.0×10^{13}	16	9.11×10^{11}	3.01×10^{6}	−1.91	−20.5	est
10	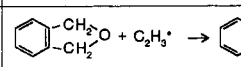	5.0×10^{12}	16	4.55×10^{9}	1.70×10^{5}	−3.05	−26.8	est
11	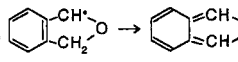	1.0×10^{13}	62	16.5	1.19×10^{12}	31	66.6	est
12	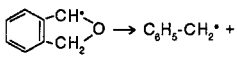	1.86×10^{16}	50	5.86×10^{6}	482	45.8	4.95	est
13	$C_6H_5–CH_3 \rightarrow C_6H_5–CH_2^{\bullet} + H^{\bullet}$	1.60×10^{15}	90	1.26×10^{-2}	3.55×10^{13}	33.8	93.9	19
14	$C_6H_5–CH_3 \rightarrow C_6H_5^{\bullet} + CH_3^{\bullet}$	5.0×10^{16}	98	1.19×10^{-2}	1.92×10^{13}	42.3	102.5	est
15	$C_6H_5–CH_3 + H^{\bullet} \rightarrow C_6H_6 + CH_3^{\bullet}$	2.40×10^{13}	5.10	2.58×10^{12}	2.72×10^{9}	3.96	−11.1	25
16	$C_6H_5–CH_3 + H^{\bullet} \rightarrow H_2 + C_6H_5–CH_2^{\bullet}$	1.20×10^{14}	8.22	3.29×10^{12}	5.30×10^{8}	6.32	−12.7	25
17	$C_6H_5–CH_2–CH_3 \rightarrow CH3^{\bullet} + C_6H_5–CH_2^{\bullet}$	6.1×10^{15}	75.1	32.4	1.89×10^{12}	41.5	78.2	32
18	$C_6H_5–CH_2–CH_3 \rightarrow C_6H_5–CH^{\bullet}–CH_3 + H^{\bullet}$	5.0×10^{15}	81	2.03	1.66×10^{14}	31.3	83.1	29
19	$C_6H_5–CH_2–CH_3 \rightarrow C_6H_5–CH_2–CH_2^{\bullet} + H^{\bullet}$	5.0×10^{15}	97	1.85×10^{-3}	6.52×10^{12}	38.4	99.8	est
20	$C_6H_5–CH_2–CH_3 + H^{\bullet} \rightarrow C_6H_5–CH^{\bullet}–CH_3 + H_2$	$4.0\times10^{-5}\times T^{5.50}$	0.33	2.36×10^{12}	1.11×10^{7}	3.91	−23.6	29
21	$C_6H_5–CH_2–CH_3 + H^{\bullet} \rightarrow C_6H_5–CH_2–CH_2^{\bullet} + H_2$	$4.0\times10^{-5}\times T^{5.50}$	0.33	2.36×10^{12}	4.78×10^{8}	11	−6.81	est
22	$C_6H_5–CH_2–CH_3 + CH_3^{\bullet} \rightarrow C_6H_5–CH^{\bullet}–CH_3 + CH_4$	3.0×10^{13}	9	5.85×10^{11}	5.09×10^{7}	−2.84	−24.6	est
23	$C_6H_5–CH_2–CH_3 + CH_3^{\bullet} \rightarrow C_6H_5–CH_2–CH_2^{\bullet} + CH_4$	3.0×10^{13}	12	1.57×10^{11}	5.92×10^{8}	4.24	−7.88	est
24	$C_6H_5–CH^{\bullet}–CH_3 \rightarrow C_6H_5–CH=CH_2 + H^{\bullet}$	3.16×10^{13}	51	6.43×10^{3}	1.71×10^{12}	30	52.5	29
25	$C_6H_5–CH_2–CH_2^{\bullet} \rightarrow C_6H_5–CH=CH_2 + H^{\bullet}$	3.16×10^{13}	35	7.06×10^{6}	4.35×10^{13}	22.8	35.8	est
26	$C_6H_5–CH_2–CH_2^{\bullet} \rightarrow C_6H_5^{\bullet} + C_2H_4$	7.0×10^{14}	43.5	3.79×10^{6}	4.22×10^{11}	31.5	36.6	est
27	$C_6H_5–CH=CH_2 \rightarrow C_6H_6 + C_2H_2$	1.58×10^{11}	58.4	1.24	9.1×10^{5}	29.4	38.5	29
28	$C_6H_5–CH_2^{\bullet} + CH_3^{\bullet} \rightarrow C_6H_5–CH=CH_2 + H_2$	2.10×10^{14}	9	4.1×10^{12}	8.74×10^{4}	−7.7	−49.2	est
29	$C_6H_6 + H^{\bullet} \rightarrow C_6H_5^{\bullet} + H_2$	1.41×10^{14}	16	1.28×10^{11}	1.12×10^{10}	10.9	6.98	21
30	$CH_4 + H^{\bullet} \rightarrow CH_3^{\bullet} + H_2$	$2.25\times10^{4}\times T^{3}$	8.8	7.41×10^{11}	4.0×10^{10}	6.74	1.07	26
31	$C_2H_4 + Ar \rightarrow C_2H_3^{\bullet} + H^{\bullet} + Ar$	3.39×10^{17}	97.3	0.111	9.20×10^{17}	35.3	114	19
32	$C_2H_4 + H^{\bullet} \rightarrow C_2H_3^{\bullet} + H_2$	5.42×10^{14}	14.9	8.0×10^{11}	3.81×10^{11}	7.88	7.36	32
33	$C_2H_4 + CH_3^{\bullet} \rightarrow C_2H_3^{\bullet} + CH_4$	$6.63\times T^{3.70}$	9.5	2.2×10^{10}	1.94×10^{11}	1.13	6.3	26
34	$C_2H_6 + H^{\bullet} \rightarrow C_2H_5^{\bullet} + H_2$	1.24×10^{14}	9.6	1.86×10^{12}	4.44×10^{9}	8.18	−4.39	19
35	$CH_3^{\bullet} + CH_3^{\bullet} \rightarrow C_2H_6$	$1.01\times10^{15}\times T^{-0.64}$	0	1.11×10^{13}	0.462	−40.4	−90.7	26
36	$CH_3^{\bullet} + CH_3^{\bullet} \rightarrow C_2H_5^{\bullet} + H^{\bullet}$	3.01×10^{13}	13.5	8.14×10^{10}	1.41×10^{14}	−4.80	11.5	32

TABLE 3 (Continued)

No	Reaction	A (s^{-1})	E (kcal)	k_f(1150 K)	k_r(1150 K)	ΔS_r(1150 K)	ΔH_r(1150 K)	Reference
37	$CH_3^\bullet + CH_3^\bullet \rightarrow C_2H_4 + H_2$	4.72×10^{15}	30.8	6.6×10^{9}	4.44	−7.55	−57	19
38	$C_2H_3^\bullet + Ar \rightarrow C_2H_2 + H^\bullet + Ar$	3.0×10^{15}	32	2.5×10^{9}	1.86×10^{16}	23.7	37.3	22
39	$C_2H_3^\bullet + H^\bullet \rightarrow C_2H_2 + H_2$	8.0×10^{13}	0	8.0×10^{13}	34.2	−3.72	−69.4	26
40	$C_2H_3^\bullet + CH_3^\bullet \rightarrow C_2H_2 + CH_4$	1.0×10^{13}	0	1.0×10^{13}	79.4	−10.5	−70.4	30
41	$C_2H_3^\bullet + HCO^\bullet \rightarrow C_2H_4 + CO$	9.0×10^{13}	0	9.0×10^{13}	7.53×10^{-3}	−10.3	−96.5	26
42	$C_2H_3^\bullet + C_2H_3^\bullet \rightarrow C_2H_2 + C_2H_4$	9.64×10^{11}	0	9.64×10^{11}	0.865	−11.6	−76.7	26
43	$C_2H_3^\bullet + C_2H_5^\bullet \rightarrow C_2H_4 + C_2H_4$	3.0×10^{12}	0	3.0×10^{12}	2.45	−10.6	−75.8	est
44	$C_6H_5{-}CH{=}CH_2 + H^\bullet \rightarrow C_6H_6 + C_2H_3^\bullet$	1.5×10^{14}	7	7.01×10^{12}	6.09×10^{11}	5.66	1.21	est
45	$C_2H_5^\bullet + H^\bullet \rightarrow C_2H_6$	3.90×10^{13}	−0.26	4.37×10^{13}	1.05×10^{-3}	−35.6	−102.2	19
46	$C_2H_5^\bullet \rightarrow C_2H_4 + H^\bullet$	3.62×10^{12}	37.2	3.1×10^{5}	2.09×10^{12}	24.7	38.2	19
47	$HCO^\bullet + Ar \rightarrow H^\bullet + CO + Ar$	2.50×10^{14}	16.9	1.54×10^{11}	1.07×10^{14}	25	17.5	22
48	$CH_3CO^\bullet + Ar \rightarrow CH_3^\bullet + CO + Ar$	1.13×10^{15}	12.3	5.20×10^{12}	4.34×10^{13}	31.1	14.4	19
49	$C_6H_5{-}CH_2{-}CH_3 \rightarrow C_6H_5{-}CH{=}CH_2 + H_2$	5.0×10^{12}	64	3.44	4.30×10^{3}	33.8	29	33

It should be added that these two reactions should not be viewed as single-step reactions although they are pictured as such in the figures. The reactions probably contain several transition states and intermediates. Since, however, these are not known, we inserted the reaction into the kinetic scheme as a single-step reaction. The rate constants for the reactions in the scheme are thus apparent rate constants. There is no way that one can invent a sequence of pathways to accurately describe the processes unless one runs quantum chemical calculations. We plan to do so sometime soon.

Whereas the first three unimolecular processes yield stable products, the fourth reaction yields unstable intermediates and is responsible for the initiation of the free radical reactions in the system. Ejection of an sp^3 hydrogen atom from C(1) or C(3) in the furan ring also initiates free radical processes. However, without the introduction of the dissociation of isodihydrobenzofuran to benzyl$^\bullet$ and HCO$^\bullet$ the calculated yields of almost all of the products are orders of magnitude below the experimental yields. Except for *o*-tolualdehyde, benzofuran, toluene, and (partially) carbon monoxide, the production of all the other products are associated with free radical reactions.

The detailed mechanism of the decomposition of isodihydrobenzofuran is reflected by the kinetic scheme shown in Table 3. As has been mentioned before free radical reactions play an important role in the decomposition. The main source for H atoms is the very fast decomposition of HCO$^\bullet$, which is formed by the unimolecular dissociation of isodihydrobenzofuran (reaction 4 in Table 3) and to a much lesser extent by the ejection of H atoms from the reactant (reaction 5). $CH_3^\bullet$ radicals are obtained by a dissociative recombination of H atoms with toluene and with *o*-tolualdehyde. The latter is also the reaction that is responsible for the presence of benzaldehyde among the decomposition products. Hydrogen atoms and methyl radicals

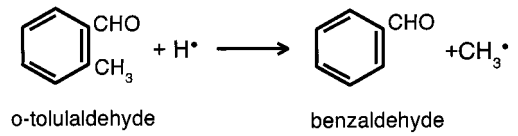

are the main chain carriers of the free radical reactions. The channel for production of ethylbenzene and styrene, for example, begins with a methyl group attack on benzyl. Figure 6 shows calculated profiles of radicals in the decomposition scheme of isodihydrobenzofuran. Benzyl radicals being very stable and products of the first generation are of the highest concentration.

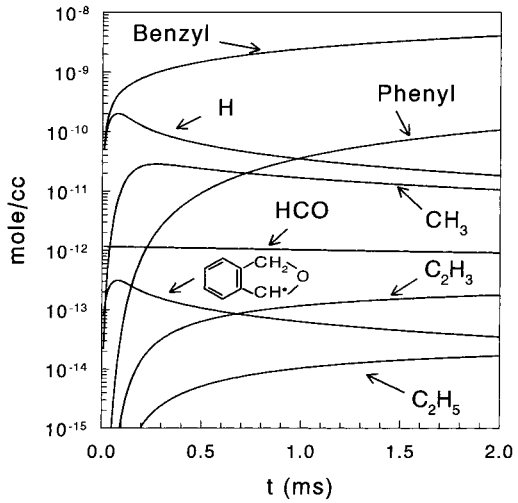

Figure 6. Calculated profiles of the important radicals in the decomposition of isodihydrobenzofuran at 1150 K.

The concentrations of HCO$^\bullet$ radicals, on the other hand, are by 3 orders of magnitude lower than those of benzyl although they are formed in the same reaction (reaction 4). This results from the extremely high decomposition rate of HCO$^\bullet$ to H$^\bullet$ and CO. The concentrations of H$^\bullet$ and $CH_3^\bullet$ are the highest among the active free radicals and are involved in the production of many products.

Reaction Scheme and Computer Modeling. To model the observed product distribution we have constructed a reaction scheme containing 26 species and 49 elementary reactions. The scheme is shown in Table 3. The rate constants listed in the table are given as $k = A\exp(-E/RT)$ (or $k = A'T^n\exp(-E/RT)$ when the rate constant fits a wide temperature range) in units of cm^3, s^{-1}, kcal, and mol^{-1}. The Arrhenius parameters for the reactions in the scheme are either estimated or taken from various literature sources, mainly from ref 19. The parameters for the reactions that were taken from ref 19 are, in many cases, best fits to a large number of entries. The thermodynamic properties of the species involved were taken from various literature sources[20−22] or estimated using ref 23 (Structure and Properties program (SP)). We performed sensitivity analysis with respect to variations (or rather uncertainties) in the ΔH^0_f of species whose thermodynamic properties were estimated or are not known accurately enough. Incorrect values of the

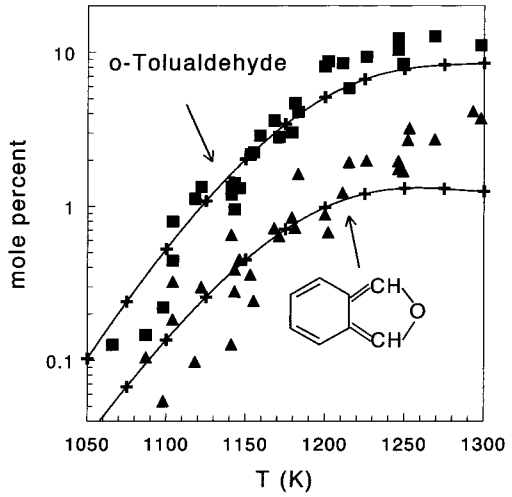

Figure 7. Calculated (lines) and experimental yields of *o*-tolualdehyde and isobenzofuran. The calculations are done at 25 K intervals, marked on the figure as crosses.

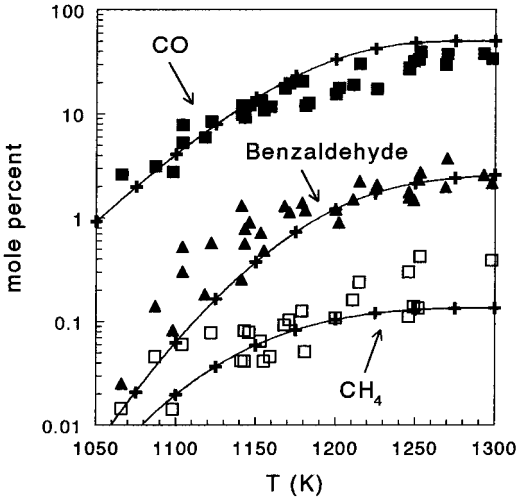

Figure 9. Calculated (lines) and experimental yields of carbon monoxide, benzaldehyde, and methane. The calculations are done at 25 K intervals, marked on the figure as crosses.

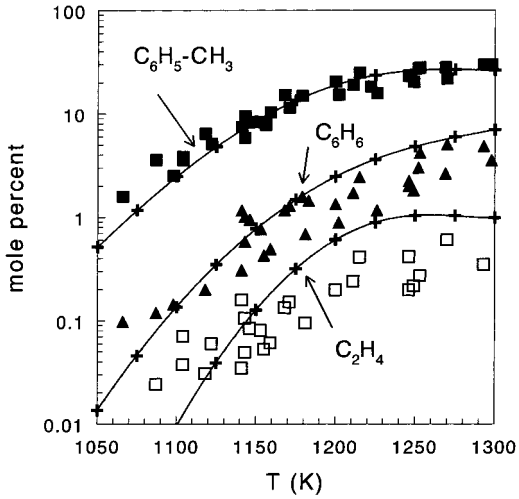

Figure 8. Calculated (lines) and experimental yields of toluene, benzene, and ethylene. The calculations are done at 25 K intervals, marked on the figure as crosses.

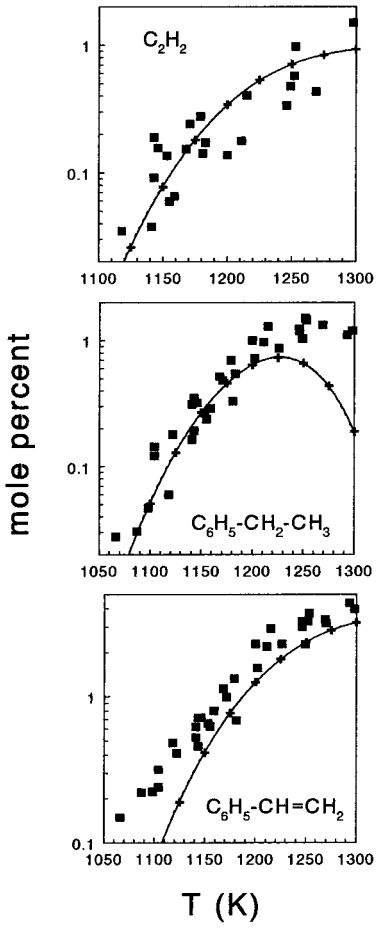

Figure 10. Calculated (lines) and experimental yields of acetylene, styrene, and ethylbenzene. The calculations are done at 25 K intervals, marked on the figure as crosses.

thermodynamic functions result in erroneous values for the rate constants of the back-reactions for a given value of the forward rate constant. In several sensitivity tests that were performed on uncertain values of heat of formation of various species, we found that the results of the computer simulations were only slightly sensitive to variations of ~3 kcal/mol in the values of the estimated ΔH^0_f.

Figures 7−10 show experimental and calculated yields of 11 products found in the postshock mixtures. Products of trace quantities were not dealt with in the scheme. The symbols in the figures are the experimental points, and the lines are the best fit to the calculated points using the scheme shown in Table 3. The calculations were made at 25 K intervals and are shown as + signs on the lines. The agreement for most of the reaction products is satisfactory.

Table 4 gives the sensitivity of the products to elimination of specific reactions from the kinetic scheme, at 1100 and 1250 K, respectively. It gives the percent change in the yield of a particular product as a result of eliminating a given reaction from the scheme. The calculations correspond to dwell times of 2 ms. Reactions that show an effect of less than 10% both at 1100 K and at 1250 K are not included in the table. A common feature to many reactions is the decreased sensitivity as the temperature increases. The number of channels that contribute to the formation of the products increase as the temperature increases and the effect of eliminating a single reaction diminishes.

Table 4 shows that only a relatively small number of elementary steps affect the product distribution in the sense that their elimination from the scheme affects the yield of at least

TABLE 4: Sensitivity Spectrum at 1100/1250 K: Percent Change in the Yields for Elimination of a Reaction from the Scheme

No	Reaction	CO	CH_4	C_2H_4	C_2H_2	C_6H_6	C_6H_5–CH_3	Iso-Benzofuran	C_6H_5–CH_2–CH_3	C_6H_5–CH=CH_2	Benzaldehyde	Tolualdehyde
1	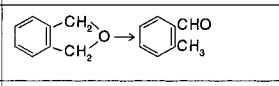	–	–28/–30	–26/–14	–26/–15	–	–	–	–26/–17	–27/–23	–99/–99	–99/–99
2	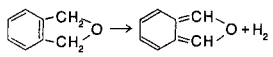	–	–	–	–	–	–	–99/–99	–	–	–	–
3	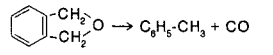	–27/–	–21/–	–	–	–37/–	–40/–17	–	–22/–	–24/–	–/28	–
4	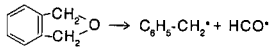	–69/–58	–94/–50	–99/–99	–99/–99	–98/–97	–50/–27	–/102	–99/–93	–99/–92	–97/–88	17/158
6	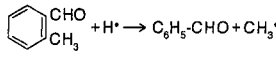	–	–28/–38	–27/–26	–26/–28	–	–	–	–26/–30	–27/–32	–100/–100	11/26
8	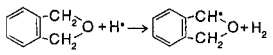	–	129/22	108/11	99	84/13	–	–	32/–	–	68/10	–
9	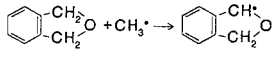	–	–94/–44	–	–	–	–	–	–	–	–	–
12	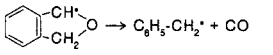	–	–	–20/–	–20/–	–	–	–	–	–	–	–
13	$C_6H_5–CH_3 \rightarrow C_6H_5–CH_2^{\bullet} + H^{\bullet}$	22/–	–/–32	512/161	516/532	71/94	–68/–90	–/–42	121/–	14/–58	207/193	–32/–84
15	$C_6H_5–CH_3 + H^{\bullet} \rightarrow C_6H_6 + CH_3^{\bullet}$	–	–65/–65	–62/–51	–62/–54	–98/–90	–	–	–64/–57	–65/–60	–	–
16	$C_6H_5–CH_3 + H^{\bullet} \rightarrow H_2 + C_6H_5–CH_2^{\bullet}$	–	23/109	26/73	25/81	23/71	–	–	13/28	–/21	13/39	–
17	$C_6H_5–CH_2–CH_3 \rightarrow CH3^{\bullet} + C_6H_5–CH_2^{\bullet}$	–	24/–11	20/–	23/13	–	–	–	–97/–96	31/–	–	–
25	$C_6H_5–CH2–CH2^{\bullet} \rightarrow C_6H_5–CH=CH_2 + H^{\bullet}$	–	–	–87/–82	14/47	–	–	–	–	19/47	–	–
26	$C_6H_5–CH_2–CH_2^{\bullet} \rightarrow C_6H_5^{\bullet} + C_2H_4$	–	–/20	–97/–95	15/54	–	–	–	–	21/54	–	–
28	$C_6H_5–CH_2^{\bullet} + CH_3^{\bullet} \rightarrow C_6H_5–CH=CH_2 + H_2$	–	66/384	–90/–61	–97/–83	–	–	–	74/283	–96/–73	–	–
38	$C_2H_3^{\bullet} + Ar \rightarrow C_2H_2 + H^{\bullet} + Ar$	–	–	10/22	–57/–66	–	–	–	–	–	–	–
44	$C_6H_5–CH=CH_2 + H^{\bullet} \rightarrow C_6H_6 + C_2H_3^{\bullet}$	–	–	–	–97/–87	–	–	–	–	–	–	–
47	$HCO^{\bullet} + Ar \rightarrow H^{\bullet} + CO + Ar$	–70/–79	–99/–99	–99/–99	–99/–99	–99/–99	–51/–62	–	–99/–98	–99/–98	–99/–98	12/24

one of the products. The majority of the elementary reactions that compose the scheme do not affect the distribution at all. They are left in the kinetic scheme for completeness and applicability beyond the temperature range of the present investigation. It should be mentioned, however, that the sensitivity analysis is performed by removing a single reaction at a time and examining its effect. When a group of reactions is eliminated from the scheme, there can be a strong effect on particular products although the elimination of only one step, as is shown in Table 4, has no affect at all. The general features of the sensitivity spectrum are self-explanatory. Removal of elementary steps that are the sole producers of a given product or are part of a consecutive chain that is the only route for a product formation reduces the concentration of that product to zero. Examples are reaction 1 for the isomerization and for the formation of benzaldehyde that is formed by dissociative recombination of H atoms with the isomerization product. Removing reaction 1 or 2 from the scheme results in the disappearance of benzaldehyde from the collection of products. Reactions 9 for methane and 17 for ethylbenzene are additional example. As has been mentioned before, many of the products are formed by free radical reactions. The most important reaction that is responsible for the initiation of free radical reaction is reaction 4 that produces $HCO^{\bullet}$. The latter decomposes practically instantaneously to CO and $H^{\bullet}$ (reaction 48). The removal of reaction 4 from the scheme reduces almost completely the concentration of all the products whose formation is associated with free radical reactions.

Differences and Similarities in the Thermal Behavior of Isodihydrobenzofuran, Dihydrobenzofuran, 2,3-Dihydrofuran, and 2,5-Dihydrofuran. Dihydrobenzofuran and isodihydrobenzofuran are two structural isomers that differ from one

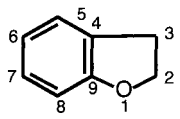

Dihydrobenzofuran

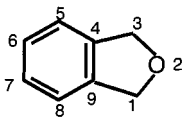

Iso-dihydrobenzofuran (Phthalan)

another in the location of the oxygen atom with respect to the benzene ring. It is of interest to compare the thermal reactions of these two isomers. It is also interesting to examine the role of the fused benzene ring on the thermal behavior of the furan ring. The thermal reactions of dihydrobenzofuran should thus be compared to those of 2,3-dihydrofuran whereas the reactions of isodihydrobenzofuran should be compared to those of 2,5-dihydrofuran. In these two molecules the fused benzene ring is removed from the molecule and is replaced by a C=C double bond.

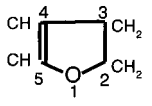

2,3-Dihydrofuran

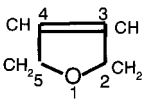

2,5-Dihydrofuran

In both dihydrobenzofuran and isodihydrobenzofuran, the bonds connecting the benzene ring to position 1 in the furan ring [oxygen atom in dihydrobenzofuran (C(9)−O(1)) and carbon atom in phthalan (C(9)−C(1)] have a partial vinylic character and are thus strong bonds (>100 kcal/mol), whereas the 1−2 bonds in both molecules are much weaker and are much more easily opened to undergo either isomerization or fragmentation.

The 1−2 bond cleavage in both molecules accompanied by H-atom migrations from C(3) to position 1 in the furan ring results in an isomerization. In dihydrobenzofuran the H atom is attached to O(1) to yield *o*-hydroxystyrene[17]

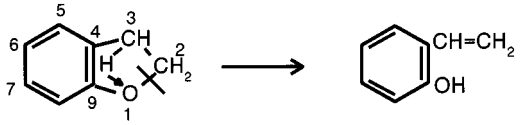

whereas in phthalan it is attached to C(1) to yield *o*-tolualdehyde. The productions of the two different isomers in the two reactants are similar processes, although preliminary DFT calculations show that the details of the potential energy surfaces of the two processes are different.[24]

In contrast to the identical isomerizations in dihydrobenzofuran and in isodihydrobenzofuran, the situation in the dihydrofuran isomers is entirely different. Whereas 2,3-dihydrofuran undergoes isomerization, 2,5-dihydrofuran does not isomerize al all. Its main reaction is a 1,6-H_2 elimination to form furan.[4,5]

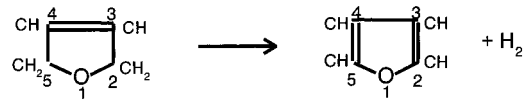

As has been mentioned before, the equivalent process in phthalan occurs also in addition to the isomerization, with relatively high yield.

The isomerization process in 2,3-dihydrofuran is different from the one in the dihydrobenzofurans. In the main isomerization process, the furan ring is cleaved to yield a 3-membered ring compound, cyclopropanecarboxaldehydele:[2]

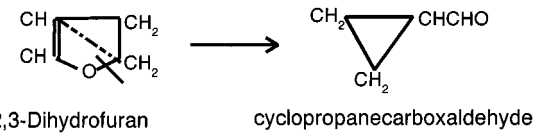

When a benzene ring is fused to the furan ring, the equivalent species that is obtained in the isomerization is unstable. In a minor isomerization process in 2,3-dihydrofuran a small amount of crotonaldehyde is also formed but the main yield of the latter is obtained by further isomerization of cyclopropanecarboxaldehydele to crotonaldehyde, in a process similar to the cyclopropane → propylene isomerization.

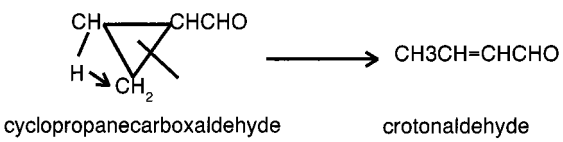

A marked difference between the dihydrofurans and the benzodihydrofurans is their kinetic stability. As expected, the benzene ring stabilizes the dihydrofuran part of the molecule and the temperature range at which the molecules begins to decompose (in the same reaction time of ~2 ms) is considerably higher, >100 K.

An important feature by which the two isomers dihydrobenzofuran and phthalan differ markedly from one another is the number of channels involving unimolecular destruction of the furan ring. This behavior is due to the fact that fragments containing oxygen atom between two carbons, which are formed during the process of phthalan decomposition, are very unstable whereas the situation in dihydrobenzofuran where the oxygen atom is at the end is considerably more stable. Thus, whereas cleavage of the ring to form benzene and ketene, dihydrobenzofuran → C_6H_6 + CH_2CO, is a major decomposition channel in dihydrobenzofuran, it does not occur at all in phthalan. No ketene was found among the decomposition products in phthalan decomposition. The main decomposition channel in phthalan is phthalan → carbon monoxide + toluene. It should be mentioned that the consecutive reactions of ketene are very important in the decomposition mechanism of dihydrobenzofuran. In 2,3-dihydrofuran the main decomposition channel is identical to that in dihydrobenzofuran where the products are ethylene and ketene, 2,3-dihydrofuran → C_2H_4 + CH_2CO.

Most of the products in the decomposition of the two isomers are the result of consecutive free radical reactions that are initiated by the unimolecular production of HCO•. Note that the concentration of CO is higher than that of toluene, particularly at high temperatures, although both are produced in equal quantities by the direct decomposition of phthalan. The reason for this behavior is that a considerable amount of the CO is produced by the very fast decomposition of HCO•, leaving after its decomposition a hydrogen atom that is the main chain carrier in the system.

Acknowledgment. This work was supported by a grant from the U.S.−Israel Binational Science Foundation under Grant Agreement No. 94-00067. We wish to thank Dr. Wing Tsang who served as the American cooperative investigator in this reaearch.

References and Notes

(1) Lifshitz, A.; Bidani, M.; Bidani, S. *J. Phys. Chem.* **1986**, *90*, 3422.
(2) Lifshitz, A.; Bidani, M. *J. Phys. Chem.* **1989**, *93*, 1139.
(3) Lifshitz, A.; Laskin, A. *J. Phys. Chem.* **1994**, *98*, 2341.
(4) Lifshitz, A.; Bidani, M.; Bidani, S. *J. Phys. Chem.* **1986**, *90*, 6011.
(5) Rubin, J. A.; Filseth, S. V. *J. Chem. Educ.* **1969**, *46*, 57.
(6) Lifshitz, A.; Bidani, M.; Bidani, S. *J. Phys. Chem.* **1986**, *90*, 5373.
(7) Organ, P. P.; Mackie, J. C. *J. Chem. Soc., Faraday Trans.* **1991**, *87*, 815.
(8) Bruinsma, O. S. L.; Tromp, P. J. J.; de Sauvage Nolting, H. J. J.; Moulijn, J. A. *Fuel* **1988**, *67*, 334.
(9) Grela, M. A.; Amorebieta, V. T.; Colussi, A. J. *J. Phys. Chem.* **1985**, *89*, 38.
(10) Laskin, A.; Lifshitz, A. Shock Waves. In *Proceedings of the 20th International Symposium on Shock Tubes and Waves, 1995*; Sturtevant, B., Sheferd, J. E., Hornung, H., Eds.; World Scientific: Singapore, London, 1996; p 971.
(11) Lifshitz, A.; Tamburu, C.; Shashua, R. *J. Phys. Chem. A* **1997**, *101*, 1018.
(12) Lifshitz, A.; Tamburu, C.; Shashua, R. *J. Phys. Chem. A* **1998**, *102*, 10655.
(13) Liu, R.; Zhou, X.; Zhai, L. *J. Comput. Chem.* **1998**, *19* (2), 240.
(14) Bouchoux, G.; Dagaut, J.; Fillaud, J.; Burgers, P. C.; Terlouw, J. K. *Nouv. J. Chem.* **1985**, *9* (1), 25.
(15) Laskin, A.; Lifshitz, A. Thermal decomposition of indene. Experimental results and computer modeling. *Proc. Combust. Inst.* **1998**, *27*, 313.
(16) Laskin, A.; Lifshitz, A. *J. Phys. Chem. A* **1997**, *101*, 7787.
(17) Lifshitz, A.; Suslensky, A.; Tamburu, C. *Proc. Combust. Inst.* **2000**, in press.

(18) Tsang, W.; Lifshitz, A. *Int. J. Chem. Kinet*. **1998**, *30*, 621−628.
(19) Westly, F.; Herron, J. T.; Cvetanovic, R. J.; Hampson, R. F.; Mallard, W. G. *NIST-Chemical Kinetics Standard Reference Database 17, Ver. 5.0*; National Institute of Standards and Technology: Washington, DC.
(20) Pedley, J. B.; Taylor, R. D.; Kirby, S. P. *Thermochemical Data of Organic Compounds*; Chapman and Hall: London, 1986.
(21) Burcat, A.; McBride, B.; Rabinowitz, M. *Ideal Gas Thermodynamic Data for Compounds Used in Combustion*; TAE 657 report; Technion-Israel Institute of Technology: Haifa, Israel, 1997.
(22) Warnatz, J. Rate coefficients in the C/H/O system. In *Combustion Chemistry*; Gardiner, W. C., Jr., Ed.; Springer-Verlag: New York, 1984.
(23) Stein, S. E.; Rukkers, J. M.; Brown, R. L. *NIST-Standard Reference Database 25*; National Institute of Standards and Technology: Washington, DC.
(24) Dubnikova, F.; Lifshitz, A. Unpublished results.
(25) Robaugh, D.; Tsang, W. *J. Phys. Chem.* **1986**, *90*, 4159.
(26) Tsang, W.; Hampson, R. F. *J. Phys. Chem. Ref. Data* **1986**, *15*, 1087.
(27) Tsang, W. *Combust. Flame* **1989**, *78*, 71−86.
(28) Brand, U.; Hippler, H.; Lindemann, L.; Troe, J. *J. Phys. Chem*. **1990**, *94*, 6305.
(29) Muller-Markgraf, W.; Troe, J. *J. Phys. Chem.* **1988**, *92*, 4914.
(30) Fahr, A.; Laufer, A.; Klein, R.; Braun, W. *J. Phys. Chem.* **1991**, *95*, 3218−3224.
(31) Kiefer, J. H.; Mizerka, L. J.; Patel, M. R.; Wei, H. C. *J. Phys. Chem*. **1985**, *89*, 2013−2019.
(32) Baulch, D. L.; Cobos, C. J.; Cox, R. A.; Esser, C.; Frank, P.; Just, Th.; Kerr, J. A.; Pilling, M. J.; Troe, J.; Walker, R. W.; Warnatz, J. *J. Phys. Chem. Ref. Data* **1992**, *21*, 411−429.
(33) Clark, W. D.; Price, S. J. *Can. J. Chem*. **1970**, *48*, 1059.